Integrated Analysis Identifies and Validates a Novel Signature Based on Immune Related Gene Predicting Survival in Bladder Urothelial Carcinoma

XuDong Mao
Zhejiang University School of Medicine Sir Run Run Shaw Hospital
ShiHan Chen
West China School of Medicine: Sichuan University West China Hospital
GongHui Li (3193119@zju.edu.cn)
Zhejiang University School of Medicine Sir Run Run Shaw Hospital https://orcid.org/0000-0001-9845-7241

Primary research

Keywords: Bladder urothelial carcinoma, Immune related gene, Immune signature, Survival, Tumor immune microenvironment

Posted Date: September 4th, 2020

DOI: https://doi.org/10.21203/rs.3.rs-71785/v1

Abstract

Background

This study aimed to develop a prognostic signature based on immune related gene(IRG) predicting survival for patients with bladder urothelial carcinoma(BLCA).

Methods

1534 IRG's expression data of 996 BLCA patients form Gene Expression Omnibus database and The Cancer Genome Atlas database were used for development and validation of the prognostic signature. Univariate Cox regression model and Random Survival Forest Variable Hunting algorithm were employed to achieve the variable selection. The independently prognostic ability of the signature was validated by Multivariate Cox model and Kaplan–Meier analysis in independent datasets. A nomogram was established to improve prognosis stratification. The relationship between tumor-infiltrating immune cells and the signature was analyzed using data retrieved from EPIC resource.

Findings

A prognostic model consisting of 10 IRGs was developed as our immune signature. Based on this signature, patients were separated into low- and high- risk groups with different survival in both training and validation sets(HR : range from 1.1 [95% CI: 1–1.2; p = 0.038] to 1.3 [95% CI: 1.3–1.5; p <0.001]). Multivariable analyses demonstrated that this signature was an independent prognostic predictor and was strongly associated with important clinicopathological factors. The signature also showed a significantly positive correlation with immune checkpoint molecules, and had a superior prognostic value compared with some important targets. In addition, our signature was found to correlate the enhancement of tumor microenvironment positively.

Conclusions

This signature predicts prognosis for BLCA patients, which may promote individualized treatment and provide potential targets for immunotherapy.

Background

Bladder urothelial carcinoma is one of the most prevalent malignancies with yearly 40 000 additional diagnoses throughout the world[1]. And transitional cell carcinoma, as the most representative pathological subtype, occupies 95% of the cancer[2]. As a highly heterogeneous disease, bladder cancer is very different on the genetic, histological, pathology and prognosis[3]. Until recently, standard therapies failed due to this complexity. Traditional treatment encompassing transurethral resection of bladder tumor or cystectomy combined with cisplatin-based chemotherapy remains the first-line regimens for patients with bladder cancer, however, the effectiveness of this treatment is still limited by staging progress, drug resistance and toxicities[4–6]. Accurate case stratification, through some biomarkers, can

promote the management of personalized treatment protocol, and likely inspire more ideal molecular therapy. Therefore, new therapeutic targets are urgently needed.

Bacillus Calmette-Guérin (BCG) early postoperative bladder irrigation after transurethral resection of bladder tumor in the prevention of recurrence of bladder tumor was considered as a classical immunotherapy, which enlighten the potential applicability of other immunomolecular therapy in bladder cancer[7, 8]. Recently, inhibitor targeting the PD-1/PD-L1 checkpoint pathway was increasingly approved for the treatment of bladder cancer[9–11]. In addition, atezolizumab (targeting PD-L1) and nivolumab (targeting PD-1) have been approved by the Food and Drug Administration (FDA) for patients with locally advanced or metastatic urothelial carcinoma[12, 13]. Howerer, according to mass of early data, the European Medicines Agency (EMA) has restricted the use of atezolizumab and pembrolizumab as a first-line treatment for urothelial carcinoma due to the reduced survival in patients with low concentrations of PD-L1 receiving either atezolizumab or pembrolizumab, suggesting that the inhibitors based on PD-L1 and PD-1 might have less effectiveness safety than conventional chemotherapy [14]. Emergence of immune checkpoint therapy including PD-1 and PD-L1 did allow the treatment of bladder cancer by reactivating immune cells cytotoxicity and sustaining immune response to become possible[15]. However, PD-1 and PD-L1 may not be the definition of the optimized immune targets, and a majority of patients do not respond to nivolumab and atezolizumab therapy. The response rate, ranging from 16–39%, regardless of the expression level of PD-1 or PD-L1, is still too low to be practical[12, 13, 16, 17]. Hence, it is imperative to develop biomarkers to monitor tumor immune environment and to improve prognostic and treatment stratification.

Many studies suggested that PD-L1 and PD-1 expression could be proposed as a prognostic marker for bladder cancer[11, 18]. High expression level of PD-L1 was more likely to be considered as advanced stage, higher grade, higher frequencies of recurrence and unfavorable prognosis[19–21]. But, observed by many studies, the clinic outcome variety could not accord with linear variation of PD-L1 expression level, suggesting that PD-L1 is an unviable signature to predict survival of urothelial carcinoma[13, 22–24]. Accumulating studies have highlighted the influence of the immune microenvironment on bladder cancer progress and immunotherapy[25]. Tumor microenvironment (TME) is composed of tumor cells, immune and inflammatory cells, tumor related fibroblasts, interstitial tissue and microvasculature[26]. Tumor microenvironment is directly influenced by the gene expression level, which called “maker gene”. The activated histiocytic components of TME will surely affect cell transcription suggesting a clinical value for immunotherapy of bladder cancer[27–29]. Therefore, the expression level of PD-L1, PD-1 and CTLA-4 might be used for measuring the different TME patterns with diverse immunohistochemistry status[18]. Therefore the expression level of IRG may act as a better biomarker to quantify the TME with a pre-existing endogenous antitumor immune response from multiple cell types, for example, “hot TME(highly infiltrated TME)” or “cold TME(non-infiltrated TME)” [30, 31].

Technically, cancers with the high mutational burden are more able to express neoantigens and might benefit more from immune checkpoint therapy because of the greater immune response mediated by T-cell. Urothelial carcinoma is such a cancer[32]. Though traditional immune checkpoints are still less than

idea, it is still believable that other IRGs could serve as more appropriate treatment or prognostic biomarkers. This investigation analyzed and explored the expression profile of IRGs to develop a novel signature that could predict clinical outcome for patients with urothelial carcinoma accurately and stably, and shed light on molecular mechanism of tumor immunology.

Methods

All statistic approaches involved in present article were conducted with R software version 3.5.2.

Publicly attainable microarray datasets and IRGs profile

The microarray datasets with clinical information were downloaded from the GEO(http://www.ncbi.nlm.nih.gov/geo/) database and the TCGA database(https://portal.gdc.cancer.gov), and only the data with complete clinical information and follow-up information were included. The RNA-seq data of GSE32894(N=224) were obtained from GEO database and used as the training set. The expression data of BLCA(N=404) were collected from TCGA database, which was used as one of the testing sets for constructing this signature. The microarray data from GSE32548(N=130), GSE13507 (N=165), GSE48075 (N=73) were also collected from the GEO database and used as testing sets. A total of 996 patients were included for analysis. The clinical and survival information of the included datasets were summarized in Table S8. The comprehensive list of IRGs containing a total of 1534 genes were downloaded from the ImmPort database (https:// immport.niaid.nih.gov)[33]. Standardization and normalization with log2 transformation were performed for the gene expression profile in each dataset using “limma” package.

Development of a Prognostic Signature

Expression microarray data from GSE32894 (N=224) was used to determine the candidate prognostic IRGs. Univariate Cox regression analysis was performed to screened out IRGs with prognostic ability as seed genes for further analyzing($p<0.01$). Random survival forest variable hunting(RSF-VH) method was employed to identify the optimal prognosis-related IRGs. In this algorithm, argument “nsplit” was set to 10, “nrep” was set to 100, “nstep” was set to 5, 1000 trees grow and the k value was set to 5[34, 35]. The importance value of each variable(IRGs) was obtained from the random survival forest. Top 10 important IRGs were remained as the optimal prognostic genes. The condition number was estimated to assess for collinearity on all variables (Table S7). Weighted by the regression coefficient, a risk score formula was established based on the expression level of each candidate prognostic IRGs, and this formula was applied to calculate every patient's risk score.

Validation of the Prognostic Signature

The median risk score was used as a cutoff point to classify patients into the high-risk group and the low-risk group. Kaplan-Meier estimate and log-rank test were employed to assess the difference in prognosis between the two groups. Univariate and multivariate Cox regression analysis were conducted to compare

the risk score with other clinical risk factors and to show its independence of other clinical predictors. A prognostic nomogram was established to predict the 3-year and 5-year DSS in GSE32894. The abilities of these nomograms were assessed with a concordance index (C-index) and calibration curves to compare the model-predicted and actual survival of DSS. Violin plot with Wilcoxon test were employed to show the association of the risk score and clinical risk factors that was significantly affect the prognosis in univariate Cox regression analysis. Correlation analysis using Pearson correlation coefficient was applied to explore the association among the IRG risk score and the expression level of immune checkpoints and several potential therapeutic targets($p<0.01$). ROC curves were used to determine the prognostic value of the risk score compared with several other signatures. In this method, patients were divided into two subgroups by different survival: longer or shorter than the median DSS, and patients surviving shorter than median DSS time of follow-up were excluded, unless death had been observed.

$p<0.01$ was considered statistically significant in univariate Cox regression analysis and correlation analysis. In the rest of method, $P<0.05$ was considered statistically significant.

The relationship of the immune signature and TME

Proportions of various infiltrating immune cell types in GSE32894 samples were retrieved from EPIC program(https://gfellerlab.shinyapps.io/EPIC_1-1/).

The abundance of immune cells including Bcells, CAFs, CD4_Tcells, CD8_Tcells, Endothelial, Macrophages and NKcells was estimated and compared between the prognostic classified risk groups using Wilcoxon test.

Geneset enrichment analysis (GSEA)

R Package “edgeR” and “limma” were used to identify differentially expressed genes (DEGs) between the high-risk group and low-risk groups form GSE32894. Based on these DEGs, Geneset enrichment analysis (GSEA) was conducted between the two group to identify potential immune-related pathways, and the results were visualized by R package “clusterProfiler”. Immunologic signatures gene sets, termed “c7.all.v7.0.symbols.gmt” including all immunologic signatures gene sets and gene symbols were used in GESA.

Results

Determination of prognostic IRGs

By utilizing univariate Cox regression analysis on GSE32894, 199 prognostic IRGs were filtered out as seek genes. Their arguments, such as regression coefficients, P values and hazard ratios have been recorded in Table S1. Random survival forest variable hunting(RSF-VH) were performed on the expression profile of these 199 IRGs for selection of the best prognostic genes. Ultimately, 30 IRGs were obtained from the random survival forest to predict DSS of patients with bladder cancer, and the top 10 important prognostic molecules were determined as model components to predict survival of patients in urothelial

carcinoma. The information of the 10 prognostic IRGs were displayed in Table 1. Figure 1A shows out-of-bag importance values for the each IRGs by bar chart. The importance calculated in Random Survival Forest Algorithm measures the increase (or decrease) in prediction error for the forest ensemble when a variable is randomly permuted in the OOB(Out-Of-Bag) samples[36, 37]. Figure S1 illustrates how these genes' expression value and patients' mortality correlate in random survival trees.

Inferentially, positive coefficients imply that the higher expression of 10 genes named TNFRSF6B, CXCL2, PSMD2, VEGFC, GRB2, CMTM1, CBL and CYR61 predict shorter survival. Negative coefficients imply that the higher levels of expression of genes called SDC1 and CTSE might predict longer survival.

Development of a prognostic signature

Based on the top 10 important IRGs, a prognostic index model was established to quantify the survival risks and the degree of immune cell infiltration in TME. The prognostic model of the weighted linear combination of the IRGs expression levels was developed, where risk score = (0.56 × expression value of TNFRSF6B) +(0.49× expression value of CXCL2) + (1.9× expression value of PSMD2) + (0.72 × expression value of VEGFC) +(1.3 × expression value of GRB2) + (1.3 × expression value of CMTM1) + (1 × expression value of CBL) + (0.64 × expression value of CYR61) + (-0.75× expression value of SDC1) + (-0.63 × expression value of CTSE). Figure 2 A-E shows that patients with higher risk score incline to have higher mortality than the other half with lower risk score in all cohorts, and patients with higher risk score tended to express a higher level of risky IRGs(TNFRSF6B, CXCL2, PSMD2, VEGFC, GRB2, CMTM1, CBL and CYR61) in their samples of tissue, whereas patients with lower risk score were more likely to express higher level of suppressor IRGs(SDC1 and CTSE).

Validation of the prognostic signature

According to the formula shown above, the risk score of each patient was calculated, and using the median risk score as a cut-off, every cohort was divided into high-risk subgroup or low risk-subgroup in same sample size respectively. For maximizing the accuracy of labeling patients with different survival risk, cohorts with odd number of samples were randomly remove one case.

Figure 3 A shows the 10-IRGs-based nomogram for 3-year and 5-year DSS predictions at different time points and the calibration curves curve in Figure 3 B and Figure 3 C shows a narrow margin between the predicted and actual values.

Figure 1B shows that the 10-IRGs-based prognostic model's C-index was 0.885 in GSE32894 for DSS; in GSE32548, it was 0.803 for DSS; in TCGA-BLCA, it was 0.624 for OS; in GSE13507, the C-indexes were 0.715 and 0.62 for DSS and OS respectively. In GSE48075, the C-indexes were 0.688 and 0.675 for DSS and OS respectively. These results all implied the predictive power of the model based on the 10-IRG signature.

As shown in Figure 4A-E, Patients of high-risk were with poor OS/DSS compared with those of low-risk in GSE32894, GSE32548, GSE13507 and TCGA-BLCA datasets, which suggested the robust predictive ability

for LUAD patients' survival outcome (log-rank test P < 0.05). In GSE48075, separate survival curves between low-risk and high-risk group were still observed despite that p value ≥0.05. Heterogeneity, batch effects, small sample size, only included MIBC specimens(Table 1) might have affected the results (Figure 4F-G).

Association with clinicopathologic factors

The univariate Cox analysis of the immune signature indicated the significant association of the signature with BLCA patients' OS in TCGA-BLCA (Hazard ratio =1.3(1.2-1.5) P < 0.001, Figure 5) and GSE13507 (Hazard ratio =1.1(1.0-1.2) P < 0.05, Figure 5) datasets, and DSS in GSE32894(Hazard ratio =1.3(1.2-1.5) P < 0.001, Figure 5), GSE32548(Hazard ratio =1.2(1.1-1.3) P < 0.001, Figure 5), GSE13507(Hazard ratio =1.2(1.1-1.4) P < 0.001, Figure 5). Clinical factors included age, T stage, G grade, pathological stage, pN, pM, cN, cM, tumor progression, whether to receive chemotherapy were observed to affect prognosis in different datasets.

Stratification analysis along with Wilcoxon test was further performed to show the association of the immune signature with these prognostic clinical factors mentioned above. In GSE32894, as shown in Figure 7A and C, patients with advanced T stage and G grade tended to have higher risk score based on the immune signature. In TCGA-BLCA cohort, as shown in Figure 7E, G and H, higher risk score was associated with higher pathologic T stage, M stage and pathological stage. As shown in Figure 7I and J, high risk score was positively related advanced T stage and G grade in GSE32548. Figure 7M, N, P, Q, R show that patients of high-risk tended to have advanced T stage, N stage, G grade, and they were under high risk of progress and more likely to have indicator of chemotherapy in GSE13507. Whereas the violin plots did not find the association of the risk score with pathological N stage in GSE32894 and TCGA datasets(Figure 7B and F). M stage and clinic N stage were not associated with risk score in GSE13507 and GSE48075(Figure 7O, T and U). And patients' Age was not observed to be related with immune signature in all corresponding cohorts (Figure 7D, L and S).

Multivariate Cox analysis further demonstrated that the immune signature could serve as an independent predictor for patients' survival of clinicopathologic factors including gender, age, T stage, G grade, N stage and M stage in GSE32894 for DSS (HR=1.26, 95%CI=1.1–1.4, P < 0.001), TCGA-BLCA cohort for OS (HR=1.4, 95%CI=1.1–1.8, P < 0.01) and GSE32548 for DSS (HR=1.13, 95% CI 1.0–1.3, P<0.05), as demonstrated in Figure 6. Whereas the novel signature didn't show its prognosis predictive independence of clinicopathologic factors in GSE13507 and GSE48075.

The Relationship between the Immune Signature and Potential Therapeutic Targets.

The correlation among CTLA4, PD-1, PD-L1, HER-2(ERBB2), ERBB3 and FRGR3 were analyzed by Pearson correlation coefficients in GSE32894. The results demonstrated that the immune signature had a negative correlation with FGFR3 and ERBB3, and a positive correlation with CD274(PD-L1), PD-1 and CTLA4 (Figure 8 A; P<0.01), but no correlation between the signature and HER-2. Compared with these targets and immune checkpoints, the ROC curves showed that the immune signature had the greatest

AUC estimated to be 0.871. This result suggested that our lncRNA signature provided better stability and reliability in predicting the DSS for patients with BLCA(Figure 8 B). Since the expression values of CTLA4, PD-1, and PD-L1 were associated with advanced tumor, correlation analysis in multiple groups were employed to figure out the relationship between the immune signature and IBC immunotherapy-related check points. As Figure 8 C demonstrated, in all five cohorts, the risk score based on this signature had a significantly positive correlation with three crucial immune checkpoints which also involved TME($p<0.01$).

Difference of Tumor-Infiltrating Immune Cells Between Groups Defined by the Signature

We analyzed the difference in tumor-infiltrating immune cells in GSE32894 samples between the high-risk group and low-risk group to detect the association of the IRG-based immune prognostic signature and the TME. Figure 9 shows that the proportions of infiltrating B cells, CAFs, CD4+Tcells, Endothelial, Macrophages were significantly enriched in the high-risk group compared to the low-risk group($p<0.01$). Consistent with these results, the proportion of other cells in tumor tissue of high-risk group was significantly decreased as compared to low-risk group($p<0.001$). The abundance of infiltrating CD8+T cells and NK cells was observed to have no obvious difference between low-risk group and high-risk group.

Determination of immune-related pathways by GSEA analysis

Grouping the patients in GSE32894 into two parts by the median risk score, the whole genome expression profile was subjected in GSEA analysis for screening immune-related pathways related to the signature. Bar plot in Figure 10 A lists the most significantly associated immune-related pathways, they are: GSE22886_NAIVE_CD4_TCELL_VS_MONOCYTE_DN, GSE22886_NAIVE_CD8_TCELL_VS_MONOCYTE_DN, GSE1460_CD4_THYMOCYTE_VS_NAIVE_CD4_TCELL_CORD_BLOOD_UP, GSE22140_HEALTHY_VS_ARTHRITIC_GERMFREE_MOUSE_CD4_TCELL_DN, GSE22196_HEALTHY_VS_OBESE_MOUSE_SKIN_GAMMADELTA_TCELL_DN, GSE22886_NAIVE_TCELL_VS_DC_DN, GSE39556_CD8A_DC_VS_NK_CELL_UP, GSE43260_BTLA_POS_VS_NEG_INTRATUMORAL_CD8_TCELL_UP.

As shown in Figure 10B, cnetplot visualizes every gene component for each immune-related pathway. Figure 10C shows the overlaps between the different immune-related pathways.

Discussion

Immunotherapy is emerging as a new anticipated therapeutic scheme for patients who are ineligible for chemotherapy due to drug resistance and toxicity. In the past few years, immune checkpoint inhibitors for bladder urothelial carcinoma have got considerable clinical survival benefits in many clinical trials and approved by FDA. Three checkpoint targets including PD-1, PD-L1 and CTLA-4 have got increasing attention for its critical role in tumor immunology mechanism and the treatment of bladder cancer. However, the expression of immune checkpoints was observed to acts as an inefficient signature to predict patients' survival and treatment response. Signature based on IRG was investigated in present

study to develop a novel biomarker to stratify patients with different survival risk and tumor immune response.

In this study, a prognostic signature consisted of 10 IRGs was developed and validated by a stepwise strategy using datasets on BLCA that retrieved from TCGA and GEO. Through a data preprocessing method, expression profiles of 1534 IRGs on 5 GEO and TCGA datasets were obtained for prognostic gene mining. Univariate Cox regression analysis was performed on GSE32894 to filter out “seed IRG” and Machine learning algorithm Random Survival Forest Variable hunting was used to capture the optimum prognostic IRGs from these candidates. Multiple methods were employed for validation of the signature’s prognostic value. The signature based on the 10 IRGs could stratify BLCA patients into two groups with statistically different survival(DSS in GSE32894, GSE32548 and GSE13507 OS in TCGA-BLCA GSE13507 and GSE48075 despite P = 0.06) with the method of Kaplan-Meier estimate and log-rank test,. Univariate Cox regression and multivariate cox regression analysis confirmed the ability to predict BLCA survival and the independence of the immune signature as compared with other clinical factors. ROC curves demonstrated that this prognostic signature had higher specificity and sensitivity than common immune checkpoints and therapeutic targets included HER-2, ERBB-3, FRGR3, PD-1, PD-L1 and CTLA-4 to serve as a prognostic biomarker. Pearson indexes of immune checkpoints and the signature in multiple cohorts were figured out by heart map, which suggested that the risk score calculated by the IRG-based formula has a positive correlation with the expression of PD-1, PD-L1 and CTLA-4. This result implied a potential substitution of the immune signature for deficient checkpoints in BLCA.

Ultimately risky IRGs including TNFRSF6B, CXCL2, PSMD2, VEGFC, GRB2, CMTM1, CBL and CYR61 and suppressor IRGs including SDC1 and CTSE were identified to be significantly associated with DSS/OS of patients with BLCA. Nomograms were provided to visualize the integrated risk score system of the signature, and C-index and calibration curves suggested the model’s superior ability to predict survival. These results all support the translational potential of this immune signature for clinical management of bladder cancer.

Yet few studies have looked into the role of IRG for survival risk categorizing and immunotherapy response estimate. Jinlong Cao et al. identified CDH7, LUZP1, PSD2, and UGT2B15 were related to survival of BLCA patients [38]. Huaide Qiu et al. demonstrated that RBP7, PDGFRA, AHNAK, OAS1, RAC3, EDNRA, and SH3BP2 classify BLCA patients into different groups with different survival rates[39]. All these reported prognostic IRGs does not overlap with the IRGs involved in the present signature.

The 10 immune genes in present study was found to be associated with tumor development and other diseases and function as inflammatory molecule in immune response. TNFRSF6B, also known as decoy receptor 3, is a member of the tumor necrosis factor receptor family, but has an absence of transmembrane and cytoplasmic domains[40]. Mounting evidences shown overexpression of TNFRSF6B in tumors is a tissue biomarker for poor prognosis in various cancers including lung and colon cancers and virus-associated lymphoma, and is a serum inflammatory biomarker associated with mortality in chronic kidney disease patients[40, 41]. Studies have demonstrated that bladder cancer (BC)

microenvironment could be regulated via CXCL2/MIF-CXCR2 signaling, and is correlated with prognosis in bladder cancer[42]. Other studied showed that blocking of CXCR2 inhibited tumor growth by decreasing the number of tumor- associated MDSCs and CCL2/CCR2 mediated myeloid suppressor cell migration in a murine tumor model[43–45]. Proteasomal non-catalytic subunit PSMD2 was found which could regulate breast cancer cell proliferation and cell cycle progression by modulating p21 and p27 proteasomal degradation and act as a potential therapeutic target in association with various clinicopathologic features in lung adenocarcinomas[46, 47]. Some miRNAs targeting VEGFC have been found to plays an important biological role in bladder cancer progress. Hirata H et al. has identified miRNA-1826 targeting VEGFC as a tumor suppressor in bladder cancer[48], Wang Y et al. suggested miR-122 as a tumor suppressor and down-regulating VEGFC expression, leading to the inhibition of bladder cancer growth and angiogenesis[49], and Yu C et al demonstrated that LncRNA PVT1 regulated VEGFC through inhibiting miR-128 in bladder cancer cells[50]. Corteggio A et al. conducted western blot analysis which has demonstrated that recruitment of growth factor receptor bound protein 2 (GRB-2) was increased in Higher grade bovine bladder carcinoma compared to normal tissues[51]. Watanabe T et al. demonstrated that Grb2 protein, transcription of GRB-2, which is the downstream effector of the EGF receptor, was substantially overexpressed in all human bladder cancer cell lines examined in comparison with cultured normal urothelial cells[52]. This paper first reported the results about the potential association of CMTM1 and CBL with BLCA. Cyr61 was found to be a molecular marker of bladder wall remodeling after outlet obstruction. Studied showed the expression of CYR61 increased with severity of BLCA progress and it could act as a molecular marker of bladder wall remodeling after outlet obstruction[53, 54]. Szarvas T et al. suggested that the overexpression of protective gene SDC1 was present in normal bladder epithelium and non-muscle-invasive cells but was absent in muscle-invasive carcinomas ($P < .001$), which was consistent with the SDC1's role of protector in present studies[55]. Wild PJ et al. performed laser microdissection and gene expression profiling and demonstrated that CTSE expression were the only factor correlated significantly with progression-free survival of pTa bladder tumors.

According to the results of GO analysis of these 10 prognostic IRGs: CTSE, PSMD2 were navigated to antigen processing and presentation; CXCL2 and CYR61 were involved in chemokine activation; CMTM1, CXCL2, CYR61, VEGFC, SDC1 and TNFRSF6B(TNFRSF6B is belong to TNF Family)were related to cytokine activity, ; GRB2 was were navigated to Natural Killer Cell Cytotoxicity and TCR signaling Pathway, CBL also was the member of TCR signaling Pathway(Table S4).

In this report, to further reveal the biological mechanisms inducing immune response involved in tumor development, GSEA listed the significantly active immune-related pathways in risky patients categorized by the immune signature. The results suggested that CD4+/CD8 + T-cell-related and NK-cell- related pathways were significantly dysregulated by the risk score based on the immune signature. Cancers with higher mutation burden, including BCLA, have a better chance of expressing neoantigens which induce greater T-cell-mediated immune response to benefit from an immunotherapy[32]. Our data showed that"Hot" TME highly infiltrated by tumor-infiltrating immune cells (TIICs) could be discriminated by the IRG-based signature accurately.

Studies demonstrated that enhanced TME influenced the gene expression of tumor tissue and related to BLCA prognosis[27, 28, 56, 57]. To further detect the predictability of the immune signature for the intensity of TME, the proportions of 7 infiltrated immune cells included Bcells, CAFs, CD4_Tcells, CD8_Tcells, Endothelial, Macrophages, NKcells were compared between different risk groups. The results supported that the prognostic signature based on IRGs could serve as a biomarker to estimate the enhancement of TME in BLCA. Since the TME significantly contributed to the mechanism by which immune check point blockade could benefit patients with advanced BLCA, this signature had provided some novel translational targets of immune response prediction and a new molecular perspective in BLCA tumor immunity.

In present study, CD4 + Tcells had a larger scale infiltration in BLCA tissue from high-risk group than low-risk group, but CD8 + had no difference. One study conducted by Liu W et al. had revealed that urothelial antigen-specific CD4 + T cells function as direct effector cells and induce bladder autoimmune inflammation independent of CD8 + T cells, which coincided with our finding[58].

The enrichment of macrophages in tumor tissue, mediated CXCL1(from same family of CXCL2), was involved in the mechanism of immune escape, tumorigenesis and angiogenesis for BLCA progression[59]. Indeed, multitype immunocytes contribute the enhancement of TME affecting survival and inflammatory response significantly and the immune signature in this study was a neo-maker identifying the clinical outcome and immunotherapy response in a predictive way. Research is still ongoing to further categorize responses, define ideal patient populations, investigate effective checkpoints and new inhibitors in clinical to seek a breakthrough way of BLCA immunotherapy. Larger-scale and prospective researches are required to validate the signature and reveal the function mechanism that merit attention.

Conclusion

10 IRGs formed a promising prognostic biomarker which could be used to distinguish patients with different survival outcome and immunotherapy response in BLCA.

And this signature also provides a series of potential therapeutic immune targets for translational medicine and improving individualized treatment.

Abbreviations

PD-1: programmed death 1; CTLA-4: cytotoxic T lymphocyte-associated antigen-4; PD-L1: programmed death ligand-1; TIM: tumor immune microenvironment; ImmPort: The Immunology Database and Analysis Portal; RNA-seq: RNA sequencing; TCGA: The Cancer Genome Atlas; GEO: the Gene Expression Omnibus; OS: overall survival; DSS: Disease specific survival; IRG: immune related gene.

Declarations

Acknowledgements

None.

Conflict-of-interest statement

The authors declare that there is no conflict of interest related to this study.

Availability of data and materials

The datasets of this article were generated from the TCGA database and the GEO database.

Institutional review board statement

This studied mined the GEO and TCGA database and doesn't involve any experiments with animals or human beings. Because the included data are a community resource project, additional ethical approval was not acquired.

Informed consent

This studied make integrated analysis based on the GEO and TCGA database, informed consent is not applicable.

Authors' contributions:

Xudong Mao designed the study, collected the literature, performed statistical analyses and analyzed the data; Shihan Chen wrote the manuscript.

Consent for publication

Not applicable.

Ethics approval and consent to participate

Not applicable.

Funding statement

There are no funders to report for this submission.

References

1. S Antoni, J Ferlay, I Soerjomataram, A Znaor, A Jemal, F Bray. Bladder Cancer Incidence and Mortality: A Global Overview and Recent Trends. European urology. 2017; 71: 96-108.
2. Xr Wu. Urothelial tumorigenesis: a tale of divergent pathways. Nature reviews Cancer. 2005; 5: 713-25.

3. C Alifrangis, U Mcgovern, A Freeman, T Powles, M Linch. Molecular and histopathology directed therapy for advanced bladder cancer. Nature reviews Urology. 2019; 16: 465-83.
4. H Von Der Maase, Sw Hansen, Jt Roberts, L Dogliotti, T Oliver, Mj Moore, I Bodrogi, P Albers, A Knuth, Cm Lippert, P Kerbrat, P Sanchez Rovira, P Wersall, et al. Gemcitabine and cisplatin versus methotrexate, vinblastine, doxorubicin, and cisplatin in advanced or metastatic bladder cancer: results of a large, randomized, multinational, multicenter, phase III study. Journal of clinical oncology : official journal of the American Society of Clinical Oncology. 2000; 18: 3068-77.
5. H Von Der Maase, L Sengelov, Jt Roberts, S Ricci, L Dogliotti, T Oliver, Mj Moore, A Zimmermann, M Arning. Long-term survival results of a randomized trial comparing gemcitabine plus cisplatin, with methotrexate, vinblastine, doxorubicin, plus cisplatin in patients with bladder cancer. Journal of clinical oncology : official journal of the American Society of Clinical Oncology. 2005; 23: 4602-8.
6. R Nadal, J Bellmunt. Management of metastatic bladder cancer. Cancer treatment reviews. 2019; 76: 10-21.
7. C Pettenati, Ma Ingersoll. Mechanisms of BCG immunotherapy and its outlook for bladder cancer. Nature reviews Urology. 2018; 15: 615-25.
8. G Redelman-Sidi, Ms Glickman, Bh Bochner. The mechanism of action of BCG therapy for bladder cancer–a current perspective. Nature reviews Urology. 2014; 11: 153-62.
9. Z Fan, Y Liang, X Yang, B Li, L Cui, L Luo, Y Jia, Y Wang, H Niu. A meta-analysis of the efficacy and safety of PD-1/PD-L1 immune checkpoint inhibitors as treatments for metastatic bladder cancer. OncoTargets and therapy. 2019; 12: 1791-801.
10. R Chen, X Zhou, J Liu, G Huang. Relationship between the expression of PD-1/PD-L1 and F-FDG uptake in bladder cancer. European journal of nuclear medicine and molecular imaging. 2019; 46: 848-54.
11. Tc Zhou, Ai Sankin, Sa Porcelli, Ds Perlin, Mp Schoenberg, X Zang. A review of the PD-1/PD-L1 checkpoint in bladder cancer: From mediator of immune escape to target for treatment. Urologic oncology. 2017; 35: 14-20.
12. Loriot Y., Rosenberg J. E., Powles T. B., Necchi A., Heijden M. Van Der. Atezolizumab (atezo) in platinum (plat)-treated locally advanced/metastatic urothelial carcinoma (mUC): Updated OS, safety and biomarkers from the Ph II IMvigor210 study. Annals of Oncology. 2016; 27.
13. Je Rosenberg, J Hoffman-Censits, T Powles, Ms Van Der Heijden, Av Balar, A Necchi, N Dawson, Ph O'donnell, A Balmanoukian, Y Loriot, S Srinivas, Mm Retz, P Grivas, et al. Atezolizumab in patients with locally advanced and metastatic urothelial carcinoma who have progressed following treatment with platinum-based chemotherapy: a single-arm, multicentre, phase 2 trial. Lancet (London, England). 2016; 387: 1909-20.
14. E Gourd. EMA restricts use of anti-PD-1 drugs for bladder cancer. The Lancet Oncology. 2018; 19: e341.
15. Vs Koshkin, P Grivas. Emerging Role of Immunotherapy in Advanced Urothelial Carcinoma. Current oncology reports. 2018; 20: 48.

16. Sl Topalian, Fs Hodi, Jr Brahmer, Sn Gettinger, Dc Smith, Df Mcdermott, Jd Powderly, Rd Carvajal, Ja Sosman, Mb Atkins, Pd Leming, Dr Spigel, Sj Antonia, et al. Safety, activity, and immune correlates of anti-PD-1 antibody in cancer. The New England journal of medicine. 2012; 366: 2443-54.
17. N Daver, G Garcia-Manero, S Basu, Pc Boddu, M Alfayez, Je Cortes, M Konopleva, F Ravandi-Kashani, E Jabbour, T Kadia, Gm Nogueras-Gonzalez, J Ning, N Pemmaraju, et al. Efficacy, Safety, and Biomarkers of Response to Azacitidine and Nivolumab in Relapsed/Refractory Acute Myeloid Leukemia: A Nonrandomized, Open-Label, Phase II Study. Cancer discovery. 2019; 9: 370-83.
18. T Kawahara, Y Ishiguro, S Ohtake, I Kato, Y Ito, H Ito, K Makiyama, K Kondo, Y Miyoshi, Y Yumura, N Hayashi, H Hasumi, K Osaka, et al. PD-1 and PD-L1 are more highly expressed in high-grade bladder cancer than in low-grade cases: PD-L1 might function as a mediator of stage progression in bladder cancer. BMC urology. 2018; 18: 97.
19. Sf Faraj, E Munari, G Guner, J Taube, R Anders, J Hicks, A Meeker, M Schoenberg, T Bivalacqua, C Drake, Gj Netto. Assessment of tumoral PD-L1 expression and intratumoral CD8+ T cells in urothelial carcinoma. Urology. 2015; 85: 703.e1-6.
20. Sa Boorjian, Y Sheinin, Pl Crispen, Sa Farmer, Cm Lohse, Sm Kuntz, Bc Leibovich, Ed Kwon, I Frank. T-cell coregulatory molecule expression in urothelial cell carcinoma: clinicopathologic correlations and association with survival. Clinical cancer research : an official journal of the American Association for Cancer Research. 2008; 14: 4800-8.
21. Ba Inman, Tj Sebo, X Frigola, H Dong, Ej Bergstralh, I Frank, Y Fradet, L Lacombe, Ed Kwon. PD-L1 (B7-H1) expression by urothelial carcinoma of the bladder and BCG-induced granulomata: associations with localized stage progression. Cancer. 2007; 109: 1499-505.
22. C Massard, Ms Gordon, S Sharma, S Rafii, Za Wainberg, J Luke, Tj Curiel, G Colon-Otero, O Hamid, Re Sanborn, Ph O'donnell, A Drakaki, W Tan, et al. Safety and Efficacy of Durvalumab (MEDI4736), an Anti-Programmed Cell Death Ligand-1 Immune Checkpoint Inhibitor, in Patients With Advanced Urothelial Bladder Cancer. Journal of clinical oncology : official journal of the American Society of Clinical Oncology. 2016; 34: 3119-25.
23. P Sharma, M Retz, A Siefker-Radtke, A Baron, A Necchi, J Bedke, Er Plimack, D Vaena, Mo Grimm, S Bracarda, Já Arranz, S Pal, C Ohyama, et al. Nivolumab in metastatic urothelial carcinoma after platinum therapy (CheckMate 275): a multicentre, single-arm, phase 2 trial. The Lancet Oncology. 2017; 18: 312-22.
24. J Bellmunt, R De Wit, Dj Vaughn, Y Fradet, Jl Lee, L Fong, Nj Vogelzang, Ma Climent, Dp Petrylak, Tk Choueiri, A Necchi, W Gerritsen, H Gurney, et al. Pembrolizumab as Second-Line Therapy for Advanced Urothelial Carcinoma. The New England journal of medicine. 2017; 376: 1015-26.
25. Ml Eich, A Chaux, G Guner, D Taheri, Ma Mendoza Rodriguez, Mdc Rodriguez Peña, As Baras, Nm Hahn, C Drake, R Sharma, Tj Bivalacqua, K Rezaei, Gj Netto. Tumor immune microenvironment in non-muscle-invasive urothelial carcinoma of the bladder. Human pathology. 2019; 89: 24-32.
26. D Hanahan, Lm Coussens. Accessories to the crime: functions of cells recruited to the tumor microenvironment. Cancer cell. 2012; 21: 309-22.

27. Ja Efstathiou, Kw Mouw, Ea Gibb, Y Liu, Cl Wu, Mr Drumm, Jb Da Costa, M Du Plessis, Nq Wang, E Davicioni, Fy Feng, R Seiler, Pc Black, et al. Impact of Immune and Stromal Infiltration on Outcomes Following Bladder-Sparing Trimodality Therapy for Muscle-Invasive Bladder Cancer. European urology. 2019; 76: 59-68.
28. Z Liu, Y Zhu, L Xu, J Zhang, H Xie, H Fu, Q Zhou, Y Chang, B Dai, J Xu. Tumor stroma-infiltrating mast cells predict prognosis and adjuvant chemotherapeutic benefits in patients with muscle invasive bladder cancer. Oncoimmunology. 2018; 7: e1474317.
29. Y Xue, L Tong, F Liuanwei Liu, A Liu, S Zeng, Q Xiong, Z Yang, X He, Y Sun, C Xu. Tumor-infiltrating M2 macrophages driven by specific genomic alterations are associated with prognosis in bladder cancer. Oncology reports. 2019; 42: 581-94.
30. M Ayers, J Lunceford, M Nebozhyn, E Murphy, A Loboda, Dr Kaufman, A Albright, Jd Cheng, Sp Kang, V Shankaran, Sa Piha-Paul, J Yearley, Ty Seiwert, et al. IFN-γ-related mRNA profile predicts clinical response to PD-1 blockade. The Journal of clinical investigation. 2017; 127: 2930-40.
31. Rf Sweis, S Spranger, R Bao, Gp Paner, Wm Stadler, G Steinberg, Tf Gajewski. Molecular Drivers of the Non-T-cell-Inflamed Tumor Microenvironment in Urothelial Bladder Cancer. Cancer immunology research. 2016; 4: 563-8.
32. M Zibelman, C Ramamurthy, Er Plimack. Emerging role of immunotherapy in urothelial carcinoma-Advanced disease. Urologic oncology. 2016; 34: 538-47.
33. S Bhattacharya, S Andorf, L Gomes, P Dunn, H Schaefer, J Pontius, P Berger, V Desborough, T Smith, J Campbell, E Thomson, R Monteiro, P Guimaraes, et al. ImmPort: disseminating data to the public for the future of immunology. Immunologic research. 2014; 58: 234-9.
34. Ishwaran Hemant, Kogalur Udaya B., Gorodeski Eiran Z., Minn Andy J., Lauer Michael S. High-Dimensional Variable Selection for Survival Data. Journal of the American Statistical Association. 2010; 105: 205-17.
35. Ishwaran Hemant, Kogalur Udaya B., Chen Xi, Minn Andy J. Random survival forests for high-dimensional data. Statistical Analysis and Data Mining: The ASA Data Science Journal. 2011; 4: 115-32.
36. Genuer Robin, Poggi Jean-Michel, Tuleau-Malot Christine. Variable selection using random forests. Pattern Recognition Letters. 2010; 31: 2225-36.
37. Ishwaran Hemant. Variable importance in binary regression trees and forests. Statistics. 2007.
38. J Cao, X Yang, J Li, H Wu, P Li, Z Yao, Z Dong, J Tian. Screening and Identifying Immune-Related Cells and Genes in the Tumor Microenvironment of Bladder Urothelial Carcinoma: Based on TCGA Database and Bioinformatics. Frontiers in oncology. 2019; 9: 1533.
39. H Qiu, X Hu, C He, B Yu, Y Li, J Li. Identification and Validation of an Individualized Prognostic Signature of Bladder Cancer Based on Seven Immune Related Genes. Frontiers in genetics. 2020; 11: 12.
40. Pitti Robert M., Marsters Scot A., Lawrence David A., Roy Margaret, Kischkel Frank C., Dowd Patrick, Huang Arthur, Donahue Christopher J., Sherwood Steven W., Baldwin Daryl T., Godowski Paul J.,

Wood William I., Gurney Austin L., et al. Genomic amplification of a decoy receptor for Fas ligand in lung and colon cancer. Nature. 1998; 396: 699-703.

41. Lin Wan-Wan, Hsieh Shie-Liang. Decoy receptor 3: A pleiotropic immunomodulator and biomarker for inflammatory diseases, autoimmune diseases and cancer. Biochemical Pharmacology. 2011; 81: 838-47.
42. H Zhang, Yl Ye, Mx Li, Sb Ye, Wr Huang, Tt Cai, J He, Jy Peng, Th Duan, J Cui, Xs Zhang, Fj Zhou, Rf Wang, et al. CXCL2/MIF-CXCR2 signaling promotes the recruitment of myeloid-derived suppressor cells and is correlated with prognosis in bladder cancer. Oncogene. 2017; 36: 2095-104.
43. Sl Highfill, Y Cui, Aj Giles, Jp Smith, H Zhang, E Morse, Rn Kaplan, Cl Mackall. Disruption of CXCR2-mediated MDSC tumor trafficking enhances anti-PD1 efficacy. Science translational medicine. 2014; 6: 237ra67.
44. B Huang, Z Lei, J Zhao, W Gong, J Liu, Z Chen, Y Liu, D Li, Y Yuan, Gm Zhang, Zh Feng. CCL2/CCR2 pathway mediates recruitment of myeloid suppressor cells to cancers. Cancer letters. 2007; 252: 86-92.
45. G Wang, X Lu, P Dey, P Deng, Cc Wu, S Jiang, Z Fang, K Zhao, R Konaparthi, S Hua, J Zhang, Em Li-Ning-Tapia, A Kapoor, et al. Targeting YAP-Dependent MDSC Infiltration Impairs Tumor Progression. Cancer discovery. 2016; 6: 80-95.
46. Y Matsuyama, M Suzuki, C Arima, Qm Huang, S Tomida, T Takeuchi, R Sugiyama, Y Itoh, Y Yatabe, H Goto, T Takahashi. Proteasomal non-catalytic subunit PSMD2 as a potential therapeutic target in association with various clinicopathologic features in lung adenocarcinomas. Molecular carcinogenesis. 2011; 50: 301-9.
47. Y Li, J Huang, B Zeng, D Yang, J Sun, X Yin, M Lu, Z Qiu, W Peng, T Xiang, H Li, G Ren. PSMD2 regulates breast cancer cell proliferation and cell cycle progression by modulating p21 and p27 proteasomal degradation. Cancer letters. 2018; 430: 109-22.
48. H Hirata, Y Hinoda, K Ueno, V Shahryari, Zl Tabatabai, R Dahiya. MicroRNA-1826 targets VEGFC, beta-catenin (CTNNB1) and MEK1 (MAP2K1) in human bladder cancer. Carcinogenesis. 2012; 33: 41-8.
49. Y Wang, Qf Xing, Xq Liu, Zj Guo, Cy Li, G Sun. MiR-122 targets VEGFC in bladder cancer to inhibit tumor growth and angiogenesis. American journal of translational research. 2016; 8: 3056-66.
50. C Yu, L Longfei, W Long, Z Feng, J Chen, L Chao, L Peihua, Z Xiongbing, C Hequn. LncRNA PVT1 regulates VEGFC through inhibiting miR-128 in bladder cancer cells. Journal of cellular physiology. 2019; 234: 1346-53.
51. A Corteggio, O Di Geronimo, S Roperto, F Roperto, G Borzacchiello. Activated platelet-derived growth factor β receptor and Ras-mitogen-activated protein kinase pathway in natural bovine urinary bladder carcinomas. Veterinary journal (London, England : 1997). 2012; 191: 393-5.
52. T Watanabe, N Shinohara, K Moriya, A Sazawa, Y Kobayashi, Y Ogiso, M Takiguchi, J Yasuda, T Koyanagi, N Kuzumaki, A Hashimoto. Significance of the Grb2 and son of sevenless (Sos) proteins in human bladder cancer cell lines. IUBMB life. 2000; 49: 317-20.

53. M Khandelwal, V Anand, S Appunni, A Seth, P Singh, S Mathur, A Sharma. RASSF1A-Hippo pathway link in patients with urothelial carcinoma of bladder: plausible therapeutic target. Molecular and cellular biochemistry. 2020; 464: 51-63.
54. D Zhou, Dj Herrick, J Rosenbloom, B Chaqour. Cyr61 mediates the expression of VEGF, alphav-integrin, and alpha-actin genes through cytoskeletally based mechanotransduction mechanisms in bladder smooth muscle cells. Journal of applied physiology (Bethesda, Md : 1985). 2005; 98: 2344-54.
55. T Szarvas, H Reis, G Kramer, Sf Shariat, F Vom Dorp, S Tschirdewahn, Kw Schmid, I Kovalszky, H Rübben. Enhanced stromal syndecan-1 expression is an independent risk factor for poor survival in bladder cancer. Human pathology. 2014; 45: 674-82.
56. Ww Lin, M Karin. A cytokine-mediated link between innate immunity, inflammation, and cancer. The Journal of clinical investigation. 2007; 117: 1175-83.
57. Lippitz Bodo E. Cytokine patterns in patients with cancer: a systematic review. The Lancet Oncology. 2013; 14: e218-28.
58. W Liu, X Chen, Dp Evanoff, Y Luo. Urothelial antigen-specific CD4+ T cells function as direct effector cells and induce bladder autoimmune inflammation independent of CD8+ T cells. Mucosal immunology. 2011; 4: 428-37.
59. M Miyake, S Hori, Y Morizawa, Y Tatsumi, Y Nakai, S Anai, K Torimoto, K Aoki, N Tanaka, K Shimada, N Konishi, M Toritsuka, T Kishimoto, et al. CXCL1-Mediated Interaction of Cancer Cells with Tumor-Associated Macrophages and Cancer-Associated Fibroblasts Promotes Tumor Progression in Human Bladder Cancer. Neoplasia (New York, NY). 2016; 18: 636-46.

Figures

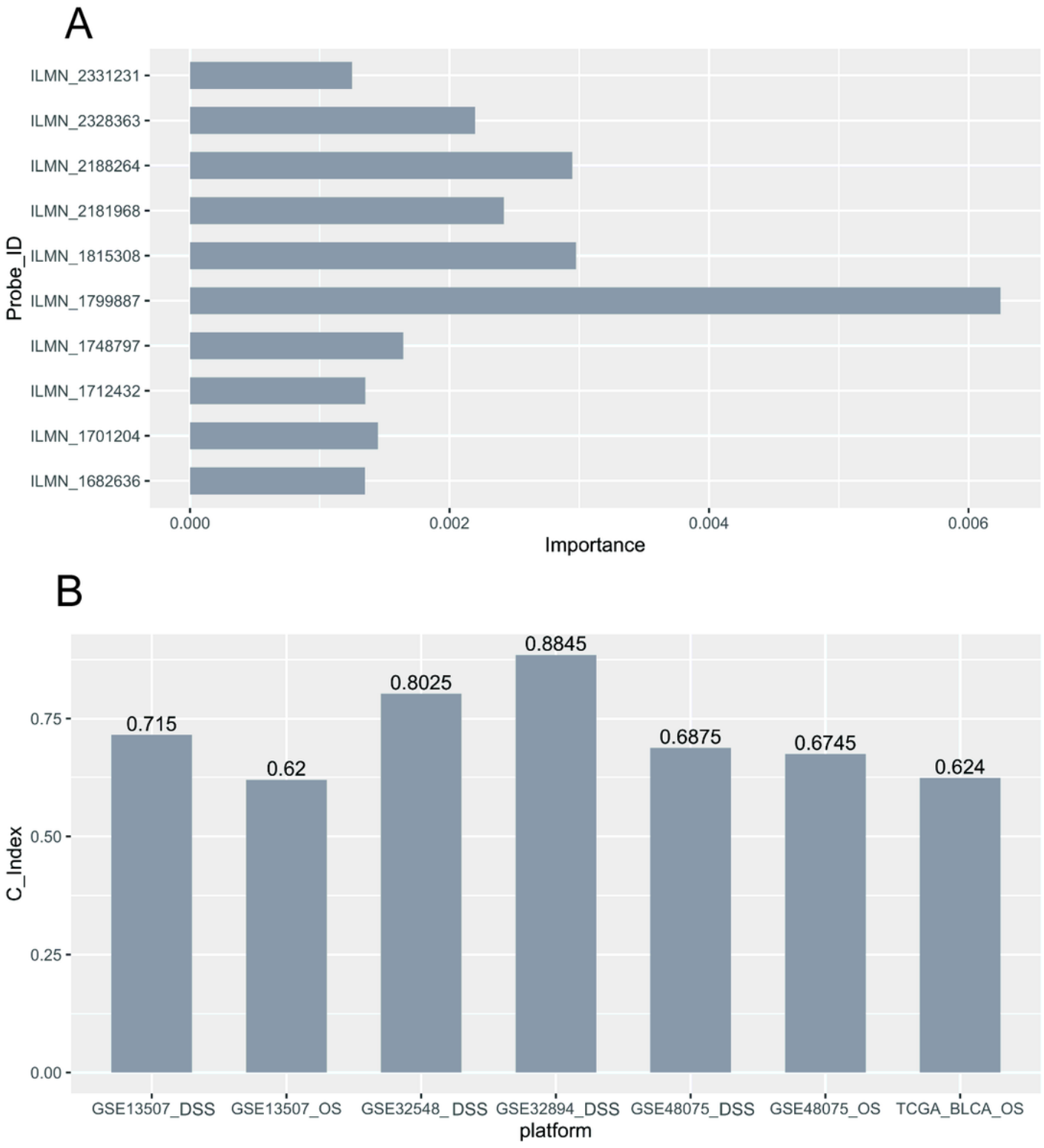

Figure 1

A, Bar chart shows the out-of-bag importance values for the each IRGs. B, Bar chart shows the C-index values for the each dataset.

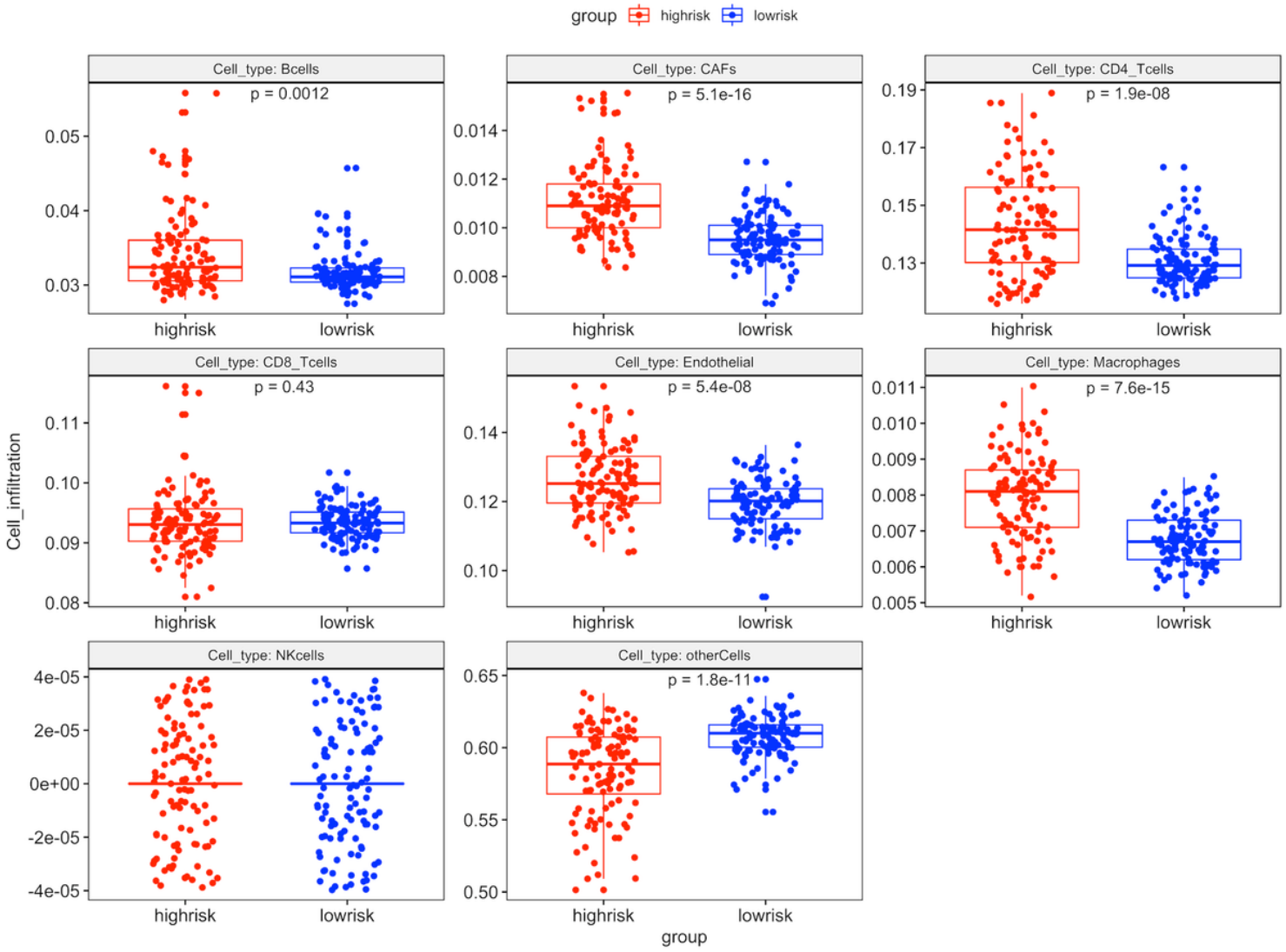

Figure 2

Patients' survival status and lncRNA expression signature were analyzed in all datasets. Scatter plots show the relationship between patients' survival status and risk score. Heatmaps of expression profiles show the relationship between gene expression level and risk score. Here, rows represent genes, and columns represent patients.

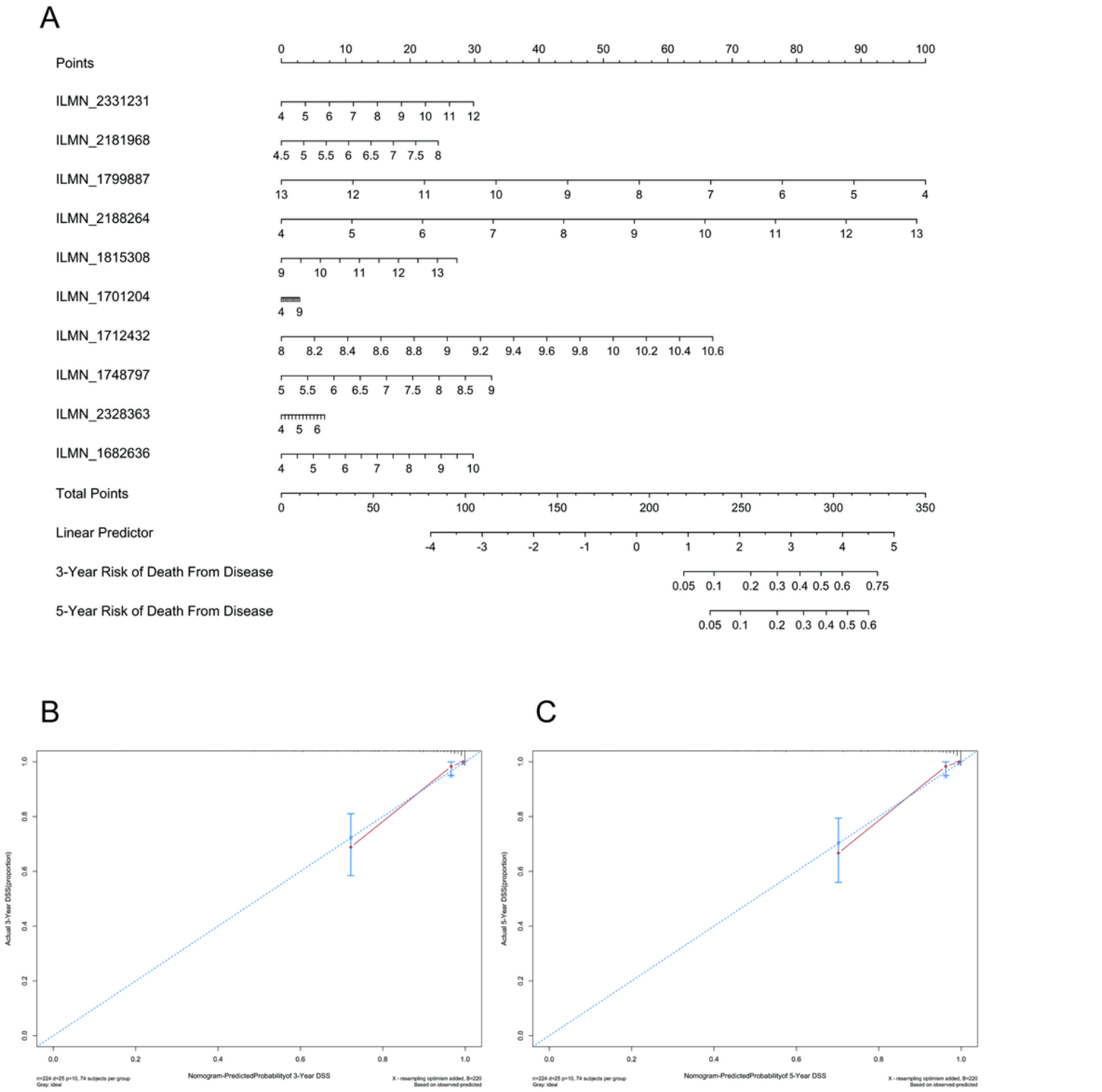

Figure 3

Nomogram to predict 3- or 5-year DSS in the GSE32894. Instructions: Locate each characteristic on the corresponding variable axis, and draw a vertical line upwards to the points axis to determine the specific point value. Repeat this process. Tally up the total points value and locate it on the total points axis. Draw a vertical line down to the 3- or 5-year DSS to obtain the survival probability for a specific BLCA patient. A, Nomogram for predicting 3- or 5-year DSS in the GSE32894 based on the the immune signature. B,

Calibration curve for the prediction of 3-year DSS assessing Nomogram in A. C, Calibration curve for the prediction of 5-year DSS assessing Nomogram in A. DSS: disease-specific survival

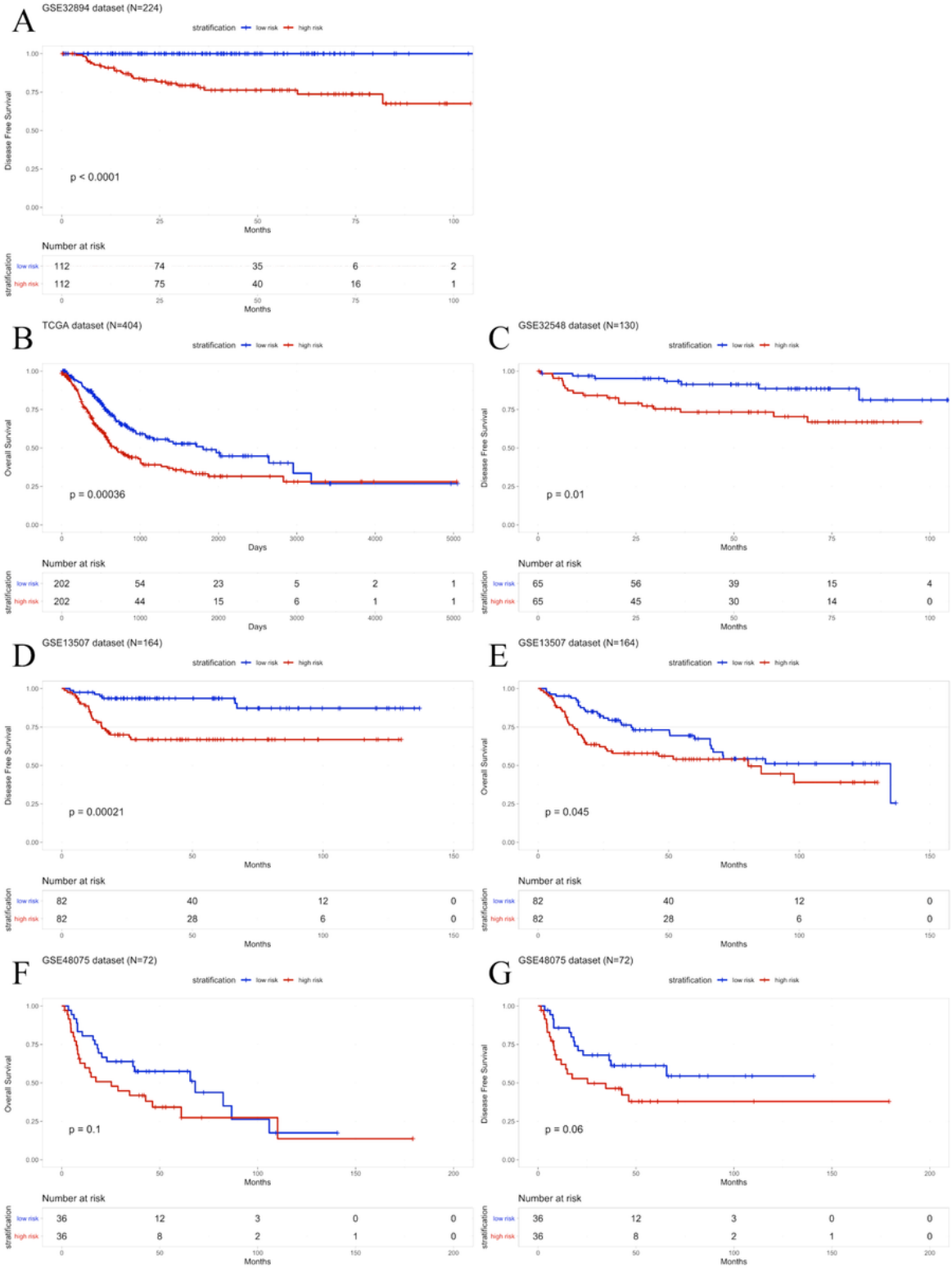

Figure 4

Kaplan-Meier estimates of the DSS or OS of BLCA patients using the immune signature. The Kaplan-Meier plots were used to visualize the DSS probabilities for the high-risk versus low-risk group of patients based on the median risk score from corresponding datasets' patents. A, Kaplan-Meier curves for

GSE32894 training series patients (N = 224) of the DSS; B, Kaplan-Meier curves for TCGA patients (N = 404) of the OS; C, Kaplan-Meier curves for GSE32548 test series patients (N = 135) of the DSS;D, Kaplan-Meier curves for the GSE13507 series patients (N = 164) of the DSS. E, Kaplan-Meier curves for GSE13507 patients (N = 164) of the OS. F, Kaplan-Meier curves for the GSE48075 series patients (N = 72) of the DSS. F, Kaplan-Meier curves for the GSE48075 series patients (N = 72) of the DSS. The tick marks on the Kaplan-Meier curves represent the censored subjects. The differences between the two curves were determined by the two-side log-rank test. DSS: disease-specific survival, OS: overall survival

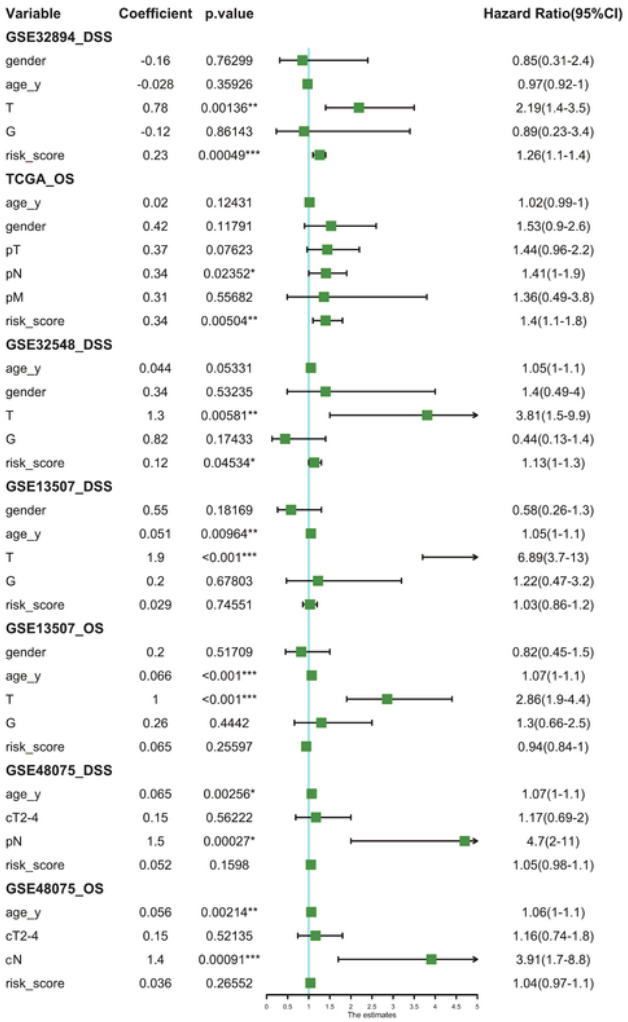

Figure 5

The Univariate Cox analysis of the signature and clinicopathological factors for GEO and TCGA datasets. TCGA: The Cancer Genome Atlas, 95% CI: 95% confidence interval, DSS: disease-specific survival, OS: overall survival

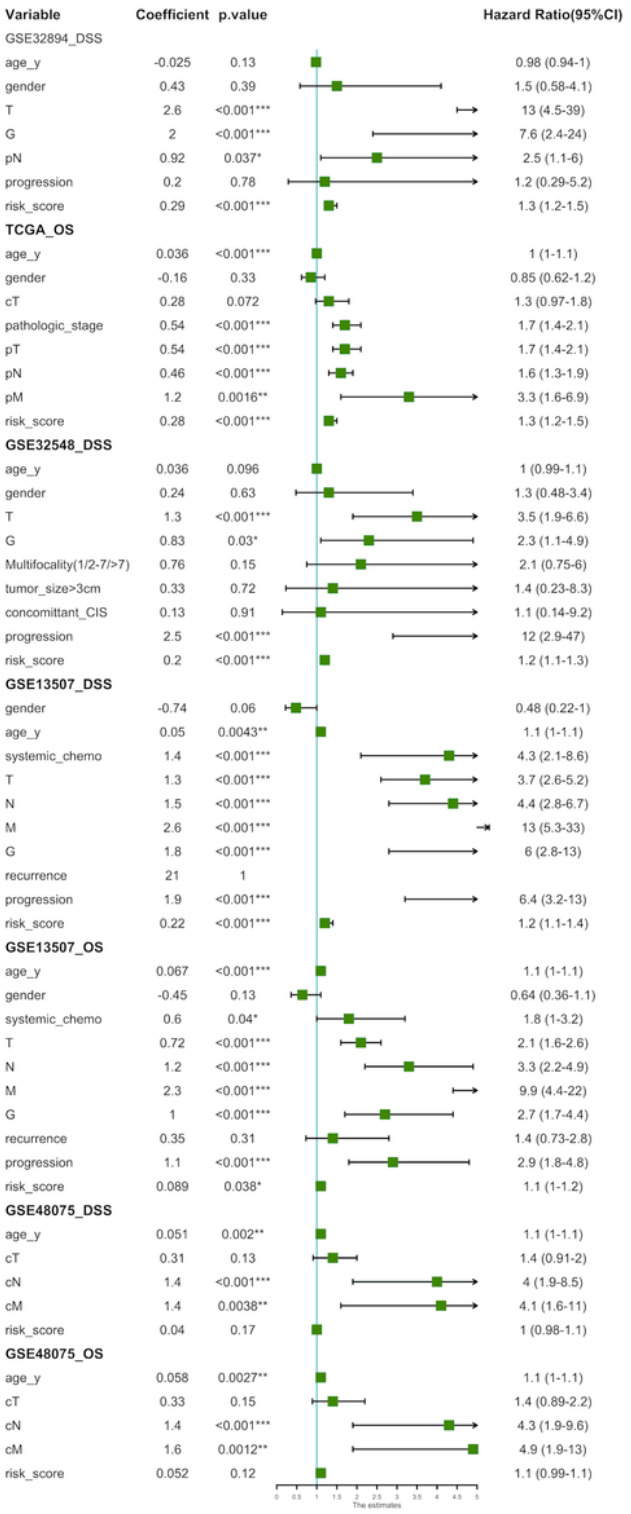

Figure 6

The Multivariate Cox analysis of the signature and clinicopathological factors for GEO and TCGA datasets. TCGA: The Cancer Genome Atlas, 95% CI: 95% confidence interval, DSS: disease-specific survival, OS: overall survival

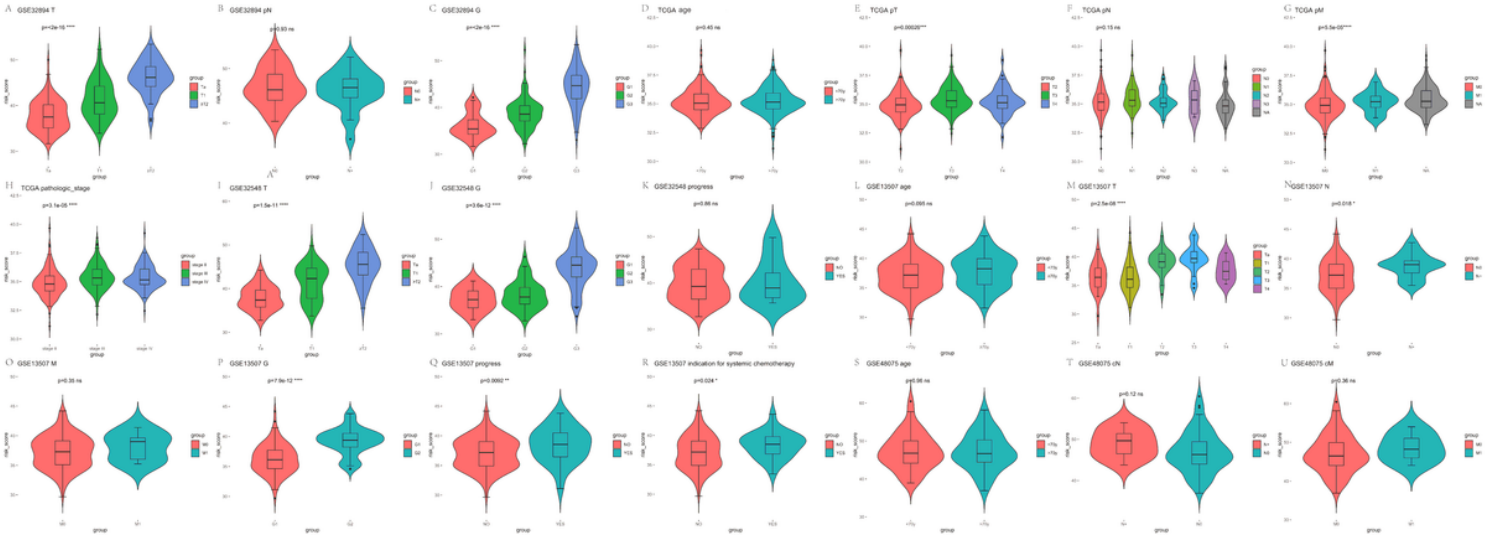

Figure 7

The relationship between the risk signature and clinicopathological factors. A Patients with high T stage tend to have higher risk scores in GSE32894 (P <0.001). B Patients with high pN stage were not observed to have higher risk scores in in GSE32894(P = 0.93). C Patients with high G grade were associated with higher risk scores in GSE32894 (P <0.001). D Patients over age 70 were not observed to have higher risk scores in TCGA dataset (P = 0.93). E Higher pT stage was associated with risk score in TCGA dataset (P <0.001). F There was no difference of the risk score between patients with different pN stage in TCGA dataset (P = 0.15). G Patients with metastasis have higher risk score in TCGA dataset (P <0.001). H Patients with higher pathologic stage were associated with higher risk score in TCGA dataset (P <0.001). I Patients with higher T stage were associated with higher risk score in GSE32548 (P <0.001). J Patients with higher G grade were associated with higher risk score in GSE32548 (P <0.001). K Patients with tumor progression was not observed to have higher risk scores in GSE32548 (P=0.86). L There was no association of the risk score with age in GSE32548 (P=0.095). M Patients with higher T stage were associated with higher risk score in GSE13507(P <0.001). N Patients with higher N stage were associated with higher risk score in GSE13507(P <0.05). O There was no association of the risk score with metastasis in GSE13507 (p=0.35). P Patients with higher G grade were associated with higher risk score in GSE13507 (P <0.001). Q Patients with tumor progression was observed to have higher risk scores in GSE13507 (P <0.01). R Patients have indication to receive systemic chemotherapy had higher risk scores in GSE13507 (P<0.05). S There was no association of the risk score with age in GSE48075 (P=0.96). T There was no association of the risk score with cN stage in GSE48075 (P=0.12). U There was no association of the risk score with metastasis in GSE48075 (P=0.36).

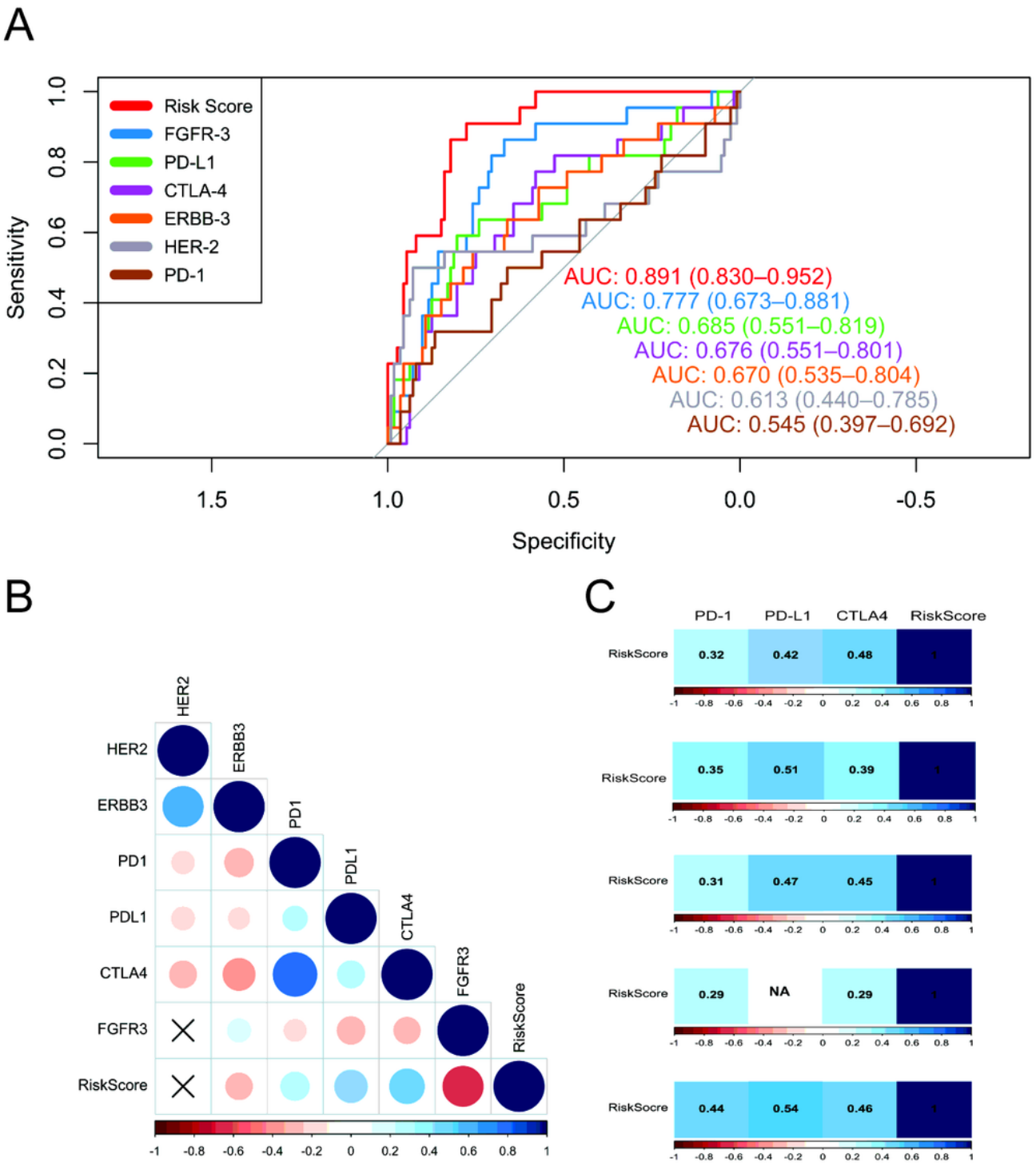

Figure 8

ROC curves and correlation analysis of different prognostic signature. A, The prognostic value of the immune signature in comparison with other prognostic molecular signature. ROC curves show that the immune signature having a largest AUC value compared with CTLA4, PD-1, PD-L1, HER-2, ERBB3 and FRGR3, estimated 0.871. B, Correlation analysis of immune checkpoints, the immune signature and potential therapeutic targets. The circle size represents P value and the color represents correlation

coefficient. Blue for positive correlation, red for negative correlation. Crosses represent p>0.01. C, Correlation analysis between the immune signature and immune checkpoints. The color and the number represent correlation coefficient. “NA” represents that the correlation coefficient was not available as p>0.01.

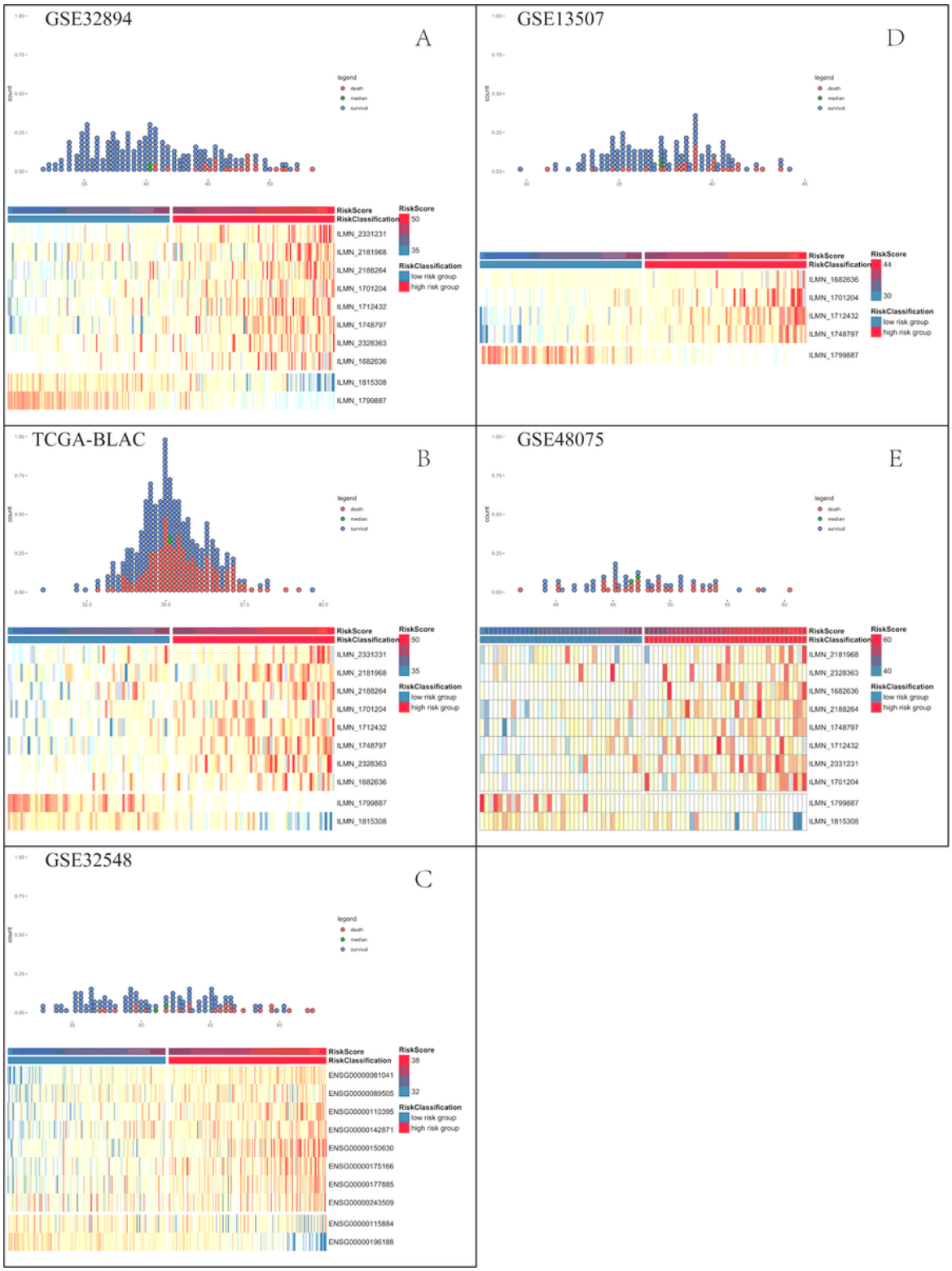

Figure 9

The difference of tumor-infiltrating immune cells among risk groups as defined by the immune-related gene (10-IRG) prognostic signature.

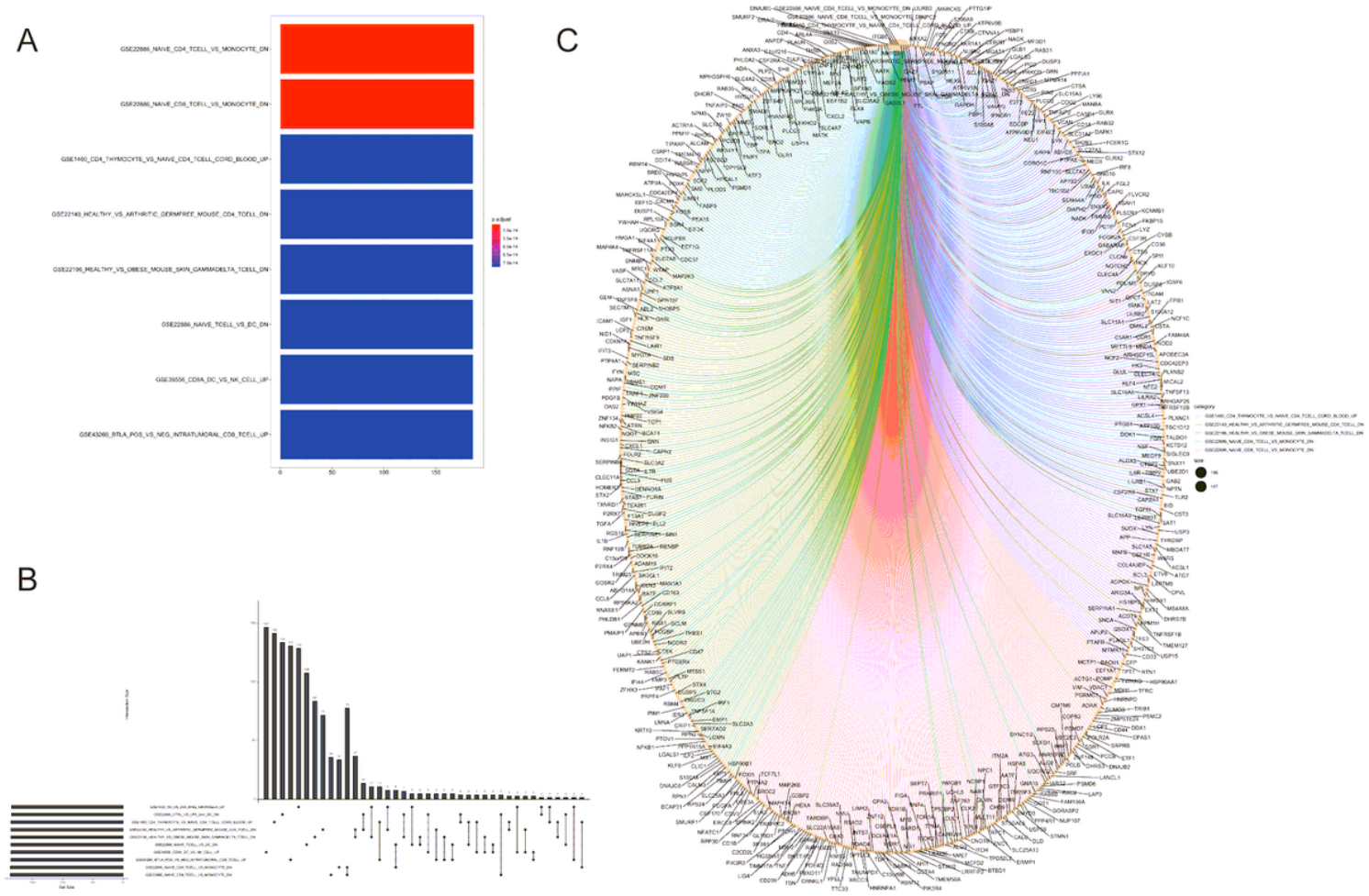

Figure 10

Results of GeneSet Enrichment Analysis (GSEA) for GSE32894. A, barplot of 6 down-regulated and 2 up-regulated immune-related pathways with minimum p value. B, Gene-Concept Network of 5 top “enriched” immune-related pathways. C, Upsetplot illustrates the overlap between top “enriched” immune-related pathways.

Supplementary Files

This is a list of supplementary files associated with this preprint. Click to download.

- TableS8.pdf
- TableS7.pdf
- TableS6.pdf
- TableS5.pdf
- TableS4.pdf

- TableS3.pdf
- TableS2.pdf
- TableS1.pdf
- FigureS1.tif